

3D Printed Prosthetic Robot Arm with Grasping Detection System for Children

Devin Babu ^{a,*}, Abdul Nasir ^a, Ravindran ^a, Mohannad Farag ^b, Waheb A. Jabbar ^c

^a Faculty of Electrical & Electronic Engineering Technology, University Malaysia Pahang, 26600 Pekan, Pahang, Malaysia

^b Faculty of Engineering/ Software Engineering Department, KARABUK University (KBU), Karabuk, 78050 Merkez Karabük, Turkey

^c School of Engineering and the Built Environment, Birmingham City University, Birmingham, West Midlands, England, United Kingdom

Corresponding author: *devinbabu@yahoo.com

Abstract—Prosthetic robot arms have been an alternative replacement for upper limb-related disability, especially among children as it helps them perform regular activities such as holding tools, eating, and drinking. This research aims to develop a 3D prosthetic robot arm using SolidWorks and 3D printer, using a low-cost and straightforward mechanism for children. This paper proposes a close loop control system with position control for the prosthetic robot arm to achieve an appropriate grasping force focusing on solid-shaped objects using PID control. The PID controller controls the system's response to perform in the most efficient path. Force-sensitive resistors (FSR) are attached to all fingers to measure the grasping force acting on objects with different surfaces, dimensions, and weights. The controller results showed improvement in the overshoot percentage of 0.902%, as overshoot is essential in preventing the grasped object's deformations. The analysis of the experiment shows that the mean grasping force and static coefficient friction of each object are different regardless of the material the object is made of and the object's mass. For example, a cube-shaped object made of wood requires 0.5288 N of grasping force to grasp the object firmly compared to a plastic-made cube that only requires 0.3245 N to hold the cube. On the other hand, the static coefficient friction for the wood cube is 3.1708 and 0.4725 for the plastic cube. Further research can be done by designing the prosthetic robot arm with independent motorized and multi-degree movement of fingers.

Keywords— Prosthetic robot arm; children; 3D printing; closed loop system; position control; PID; FSR sensor; grasping force.

Manuscript received 27 Oct. 2021; revised 24 Apr. 2022; accepted 6 Jun. 2022. Date of publication 28 Feb. 2023.
IJASEIT is licensed under a Creative Commons Attribution-Share Alike 4.0 International License.



I. INTRODUCTION

Recent years have seen a rise in cases seeking support for physical disabilities by individuals suffering from permanent impairment or loss of limbs due to trauma, injury, and congenital conditions [1]. According to the WHO, 2.4 million of 3 million upper limb patients are middle class [2]. This prediction suggests that around 160,000 of the current 32 million Malaysian population need prosthetic or orthotic equipment. In Malaysia, the prevalence of amputations has risen, with many significant service components that offer aspects such as service interference that meet the increasing demand. However, there are barriers to providing prosthetic services in Malaysia from multiple elements, such as the financial burden of obtaining prosthetics and the lack of expertise in producing quality prostheses. Prosthetic equipment is a widely used instrument in modern technology [3], especially in medicine and the healthcare system. Robotic prostheses have a high market value today [4], and most

research is being developed in this field. In the last decade, academia and industry have come with significant research to advances in technology use, such as the implementation of deep learning, embedded controllers, brushless motors, and lithium batteries to increase the performance of the prosthetic device. The prosthesis is divided into several types [5]. The primary type is myoelectric, endoskeleton, exoskeletal, and body-driven prosthesis. A myoelectric prosthesis uses biological signals to shift the prosthetic limb. Electrodes are applied to the muscle [6] to monitor the action potential, and sensors are designed to receive electrical alerts inside the fabricated socket.

Children's prosthesis needs are problematic regarding children's growth rates, where access to prostheses significantly impacts psychosocial development [7]. Although existing device supports cosmetics, consumer features are not available to children due to high prices from a low-income [8] family or developing country cannot afford beyond a prosthetic robot arm installed with simple grippers, insurance plans, medical availability, and their perceived

reliability [9] and control complexity. Although there is rapid growth in the 3D [10] prosthetic industry, there are no proper guidelines and overview of all prosthetics designed and printed. Most scientific research [11] ongoing in upper limb 3D prostheses is done by trial and error, where the obstacle is to design a 3D prosthetic that is identical in terms of the weight and size of the replaced limb [12]. Evidence of the existing functional performance of the 3D prosthetic robot arm from customers is lacking in rating the prosthetic.

Numerous prosthetic robot arm that is available does not have the regenerative potential of a real human hand [13], and the intricate interplay of intuitive motor control, proprioception, and touch that is the hallmark of human upper limb function has yet to be discovered. The main problem in performing a stable grasp [14] of a prosthetic robot arm is real-time detection of an object slippage during grasping with a small motor tends to overdamp the hand and increase the time of hand opening. An accurate grasping force like a human finger cannot be achieved, although plenty of decoding methods were being used [15] and tested to prevent slippage of the grasped object. Even if this decoding method feedback can simulate a real-human hand [16], the time delay of grasping an object would be longer than the nature hand [17]. Although there are many prosthetics available, there is still a significant gap compared to human hands due to the absence of a feedback system [18] in prostheses compared to humans, where it has numerous sensory receptors that as feedback to the central nervous system [19] while the prostheses only operate in open loop system without feedback. Most prostheses do not restore sensory feedback like tactile sensors or sophisticated control [20].

II. MATERIAL AND METHOD

A. Proposed Design and Components

The design of the children's prosthetic robot arm is obtained from the previous study [21]. The research designed children's prosthetic robot arms using Styrofoam material. The dimension of the prosthetic robot arm designed in this research is in Fig 1. The overall design of the hand is in Fig. 1. The design of the 3D prosthetic robot arm is converted to an STL file and printed using Creality software. The material used to print is PLA, which is light in weight. Fig.2 shows the prosthetic robot arm's fingers, Fig.3 shows the forearm piece of the prosthetic robot arm, and Fig.4 shows the palm piece of the prosthetic robot arm previously designed in SolidWorks.

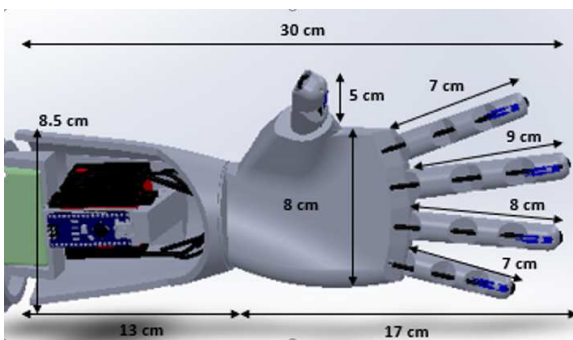


Fig. 1 Overview of the prosthetic robot arm

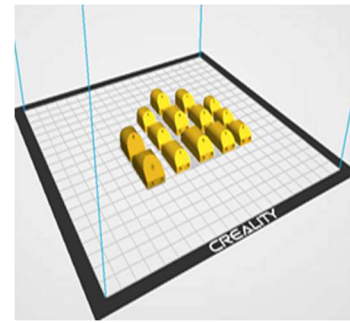


Fig. 2 Fingers of the prosthetic robot arm

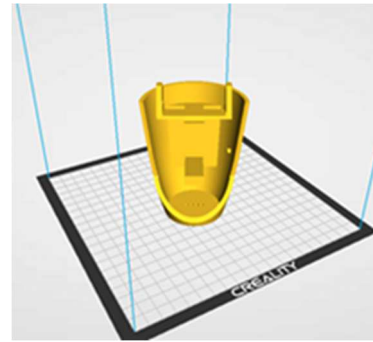


Fig. 3 Forearm piece of the prosthetic robot arm

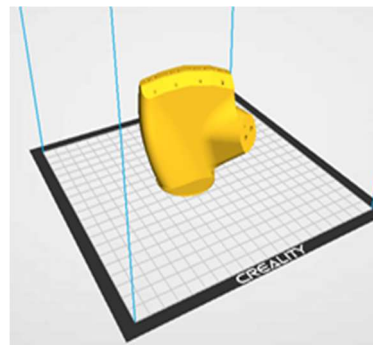


Fig. 4 The palm piece of the prosthetic robot arm

B. Components

Table 1 shows the list of the components that is suitable for installation in the prosthetic robot arm. The details of each component are as below.

TABLE I
DETAILS OF COMPONENTS WITH SPECIFICATION

Devices	Specification
 FSR Sensor	i. Shape: Flexible ii. Output signal: analog iii. Pressure induction range: 10 g-1000 g iv. Size: 5mm*20mm / 0.197in*0.787in
 Servo Motor	i. Speed (sec/60deg): 0.10/4.8V ii. Torque (Kg-cm): 10/6V iii. Size (mm): 40.7mm x 19.7mm x 42.9mm iv. Rotation angle: 180 degree

Devices	Specification
 <p>Arduino Mega 2560</p>	i. ATmega2560 ii. Operating Voltage: 5V iii. Input Voltage 7-12V iv. Digital I/O Pins: 54 v. Analog Input Pins: 16
 <p>Lipo Battery</p>	i. Capacity: 1100mAh ii. Continuous discharge rate: 25C iii. Voltage: 11.1V iv. Weight: 85g

1) *Arduino Mega 2560*: The Arduino Mega 2560 is a microcontroller board based on the ATmega2560. It has 54 digital input/output pins (15 can be used as PWM outputs), 16 analog inputs, 4 UARTs (hardware serial ports), a 16 MHz crystal oscillator, a USB connection power jack, an ICSP header, and a reset button [22]. It contains everything needed to support the microcontroller; simply connect it to a computer with a USB cable or power it with an AC-to-DC adapter or battery to get started. The Mega 2560 board is compatible and flexible [23], with most shields designed for the Uno and the former boards, Duemilanove or Diecimila.

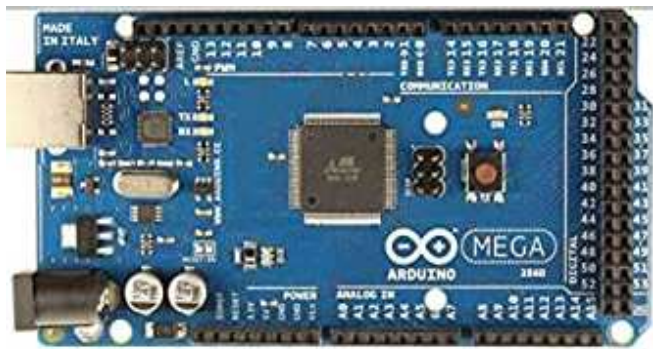


Fig. 5 Arduino Mega 2560

2) *FSR Sensor*: A force sensor can be installed at the fingertip to detect the amount of force the servo motor applies on the grasped object [24] to prevent slipping. The sensor's resistance decreases as the pressure on the film increase. The pressure sensing range of the sensor is 10 g to 1 kg, and the thickness of 0.255 mm, which is suitable to be installed on the area [25] of the fingertip of the prosthetic robot arm. The FSR needs to calibrate with a voltage divider circuit, as in Figure 7, before achieving an accurate measurement.



Fig. 6 FSR sensor

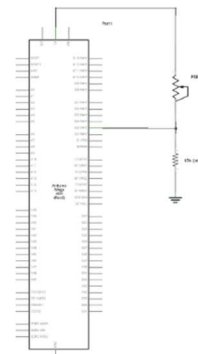


Fig. 7 FSR calibration circuit

3) *Servo Motor* Tiny and lightweight with high output power. The servo can rotate approximately 180 degrees (90 in each direction) and works just like the standard but more miniature [26]. It is suitable to make stuff move without building a motor controller with feedback [27] and a gearbox, especially since it fits in small places. It comes with three horns (arms) and hardware.



Fig. 8 Servo Motor

4) *Lipo Battery*: The most successful product in battery technology production, the lithium-ion (LiPo) battery has the most established used battery for all general purposes [28]. A rechargeable 11.1 V, 1100 mAh LiPo battery is suitable [29] to be used as the power source of the prosthetic arm as the Arduino. The servo motor only requires an input power supply of less than 10 V. A fully charged LiPo battery chargers up to 12.6 V with the maximum rate of discharge of 25 C, and LiPo batteries are light in weight, 100 g, and rechargeable as it is easy to install and recharge.

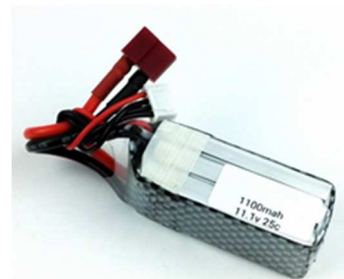


Fig. 9 Lipo-Battery

The maximum operating hours of the battery, the capacity of the battery and the total amount of current from the connected load must be determined. As in this research, Arduino Mega with 200 mA and the servo motor with 250 mA current are supplied from the battery with a 2200 mAh. To determine the operating hours, $T_{Battery}$ the equation (1) can be used to estimate the hours of operating:

$$T_{Battery} = \frac{C_{mAh}}{I_{load}} \quad (1)$$

It can be formulated as below by substituting the details of the load.

$$T_{Battery} = \frac{2200 \text{ mAh}}{500 \text{ mA} + 500 \text{ mA} + 70 \text{ mA}} \quad (2)$$

$$T_{Battery} = 2.056 \quad (3)$$

$$T_{Battery} = 2 \text{ hours } 3 \text{ minutes} \quad (4)$$

The operating hours of the battery with maximum continuous load current are 2 hours 3 minutes, as estimated from the equation above.

C. Mathematical Modelling

According to a previous study, the force from the servo is applied toward the fingers' flexion movement, where the hand's behaviour is compared to the simplified cantilever beam model. The study resulted in two equations of actuator applied force and reaction force as below.

$$\delta_a = \frac{f_r * h * l^2}{2 * E * I} \quad (5)$$

where:

δ_a	tension on the tendon	Nm^{-1}
f_r	force due to the tension on the string	N
h	radius of the shaft to the tendon	m
l	length of the string	m
E	Young's modulus of the material	Nm^{-2}
I	The second moment of the area	m^4

$$\delta_r = \frac{F_t * l^3}{3 * E * I} \quad (6)$$

where:

δ_r	Force detection due to reaction force	N
F_t	Total force of actuator and reaction force	N

By solving equations (2) and (3), it can be obtained as below.

$$F_t = \frac{3 * f_r * h}{2 * l} \quad (6)$$

where:

F_t	Fingertip force	N
-------	-----------------	---

1) *Control System*: Figure 10 shows the proposed controller in this work. The desired angle position is the controller's input, and the finger flexion angle is the output. A PID controller is used to tune the controller as K_p , K_i , and K_d gains can be adjusted for the system's optimum operations. The PID controller consists of three parts: proportional, integral, and derivative.

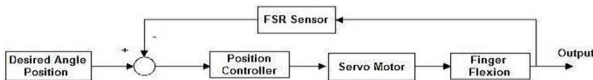


Fig. 10 Block diagram of the prosthetic robot arm

The proportional is for removing a large amount of error in the system. The necessary action is to reduce the steady-state error or offset. The derivative functions are to reduce the system's overshoot. The PID equation is as below:

$$u(t) = K_c \left[e(t) + \frac{1}{\tau_i} \int e(t) dt + \tau_D \frac{d e(t)}{dt} \right] \quad (8)$$

where:

$u(t)$	control signal
$e(t)$	error signal
K_c	proportional gain
τ_i	integral time
τ_D	derivative time

2) *Mathematical Modelling of Servo motor*: The electric motor block in Simulink is used to replace the servo motor as there is no servo motor block in Simulink. However, the equation inside the block is modified according to the servo motor transfer function as in Equation 9.

$$\frac{\theta(s)}{V_a(s)} = \frac{K_{tn}}{(s*L+R)[(J_{eff}*s^2)+(f_{eff}*s)]+s*K_{tn}*K_b} \quad (9)$$

where:

R	armature resistor	Ω
L	armature inductance	H
K_b	constant of back voltage	V
$V_a(s)$	applied armature voltage	V
$\theta(s)$	motor position (angular)	rad
J_{eff}	moment inertia motor	$\text{kg} * \text{m}^2$
f_{eff}	coefficient viscous motor and load	$\text{N} * \text{m} * \text{s}$

3) *FSR Sensor*: The force value from the FSR sensor, F_n is compared at the summing point with a signal generator and force control model to measure the applied force on the object by grasping the fingers. The model measures the grasped force value of the FSR sensor value and the servo motor force value. The Equation as below

$$\Delta F = F_{Grasp} \quad (10)$$

There is five FSR sensor attached to each finger of the prosthetic robot arm. To calculate the FSR resistance value in Newton, first the supply voltage, V_{cc} and analog voltage, V_o need to be determined as the supply voltage for the FSR sensor is 5V, and analog voltage is based on the sensor output when there is a contact on the sensor surface. A voltage divider circuit, a pull-down resistor, R of 10k ohm, is placed. The equation of the voltage divider is as below.

$$FSR \text{ resistance} = \frac{((V_{cc} - V_o) * R)}{V_o} \quad (11)$$

The conductance of the sensor is calculated based on the FSR resistance as the conductance G is reciprocal to the sensor's resistance.

$$G = \frac{1}{FSR \text{ resistance}} \quad (12)$$

The coefficient of friction is determined by the grasping force for each object that is grasped by the hand. The friction ratio is labeled as static coefficient friction, as in Equation (9).

$$\mu_s = \frac{F_t}{m * g} \quad (13)$$

where:

μ_s	static coefficient friction	
F_t	total force of actuator and reaction force	N
m	mass of grasped object	kg
g	gravitational force	m s^{-2}

D. Selection of Grasped Objects

There is various grasping type for lifting an object. Therefore the suitable type is selected based on the shape of an object referred to in the journal by [30]. The prosthetic robot arm is developed for children; hence, children's common objects in daily life are used in the experiment testing. The list of the object that is grasped is in the figures below.

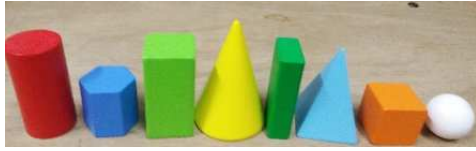


Fig. 11 Solid wood made regular-shaped objects

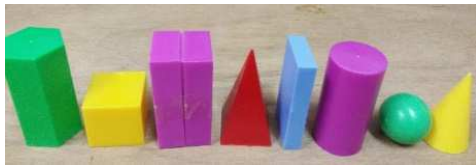


Fig. 12 Solid plastic made regular shape objects



Fig. 13 Random objects

Fig.11 shows solid regular shape objects made of wood, and Fig.12 shows plastics made of solid regular shape objects. Both types of objects are used in the grasping experiment. On the other hand, Fig.13 shows random objects with random object-made material used in the grasping experiment. The solid and plastic objects' mass is in TABLE II below.

TABLE II
DETAILS OF OBJECTS WITH MASS

Part	Mass (g)
Puzzle Piece	54
Cylinder container	70
Mini Book	107
Solid Cube	34
Plastic Ball	3
Duck Toy	8
Plastic Cube	7
Plastic Cylinder	11
Plastic Hexagon	23
Plastic Pyramid	14
Plastic Rectangular	10
Plastic Square	6
Wood Cube	17
Wood Cylinder	17
Wood Hexagon	32
Wood Pyramid	13
Wood Rectangular	26
Wood Square	18

III. RESULTS AND DISCUSSION

A. Construction of 3D Printed Prosthetic Robot Arm

The designed model in SolidWorks is then printed using a 3D printer. The thumb, index, middle, ring, and ring finger are printed using PLA material which took 28 hours of total printing time. The right palm required a total of 32 hours of total printing time. The fingers are connected internally using nylon strings of 0.7 mm diameter. The nylon-string flows through the fingertip to the palm and the servo motor shaft, which is knotted with the knob. Two servo motor of stall torque 8.5 Nm is placed on the forearm of the prosthetic robot arm. Table III shows the dimension of the thumb, index, middle, ring, pinky, palm width, and forearm width are 5 cm, 7 cm, 9 cm, 8 cm, 7 cm, 8 cm, and 8.5 cm, respectively.

TABLE III
DIMENSION OF THE PROSTHETIC ROBOT ARM

Part	Dimension (cm)
Thumb	5
Index Finger	7
Middle Finger	9
Ring Finger	8
Pinky Finger	7
Palm	8
Forearm	8.5



Fig. 14 Printed right-hand fingers



Fig. 15 Printed right-hand palm



Fig. 16 Fully assembled 3D prosthetic robot arm



Fig. 17 3D prosthetic robot arm with FSR sensor attached

B. Controller

The MATLAB'S Simulink system resulted in the controller response as in the graph below:

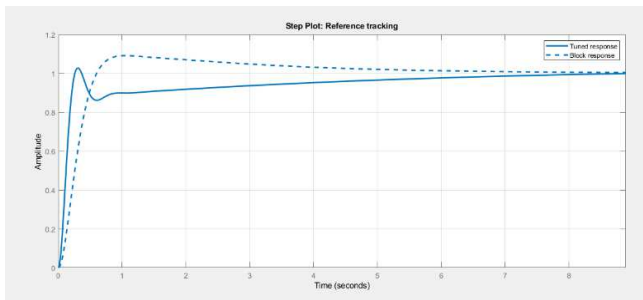


Fig. 18 Step Plot of the system

The graph above in Fig 18 shows the step plot of the PID response system. The tuned has a slower rise time than the block, but the settling time requires extra time compared to the block settling time.

TABLE IV

STEP RESPONSE PARAMETERS OF THE TUNED AND BLOCK CONTROLLER

Parameters	Rise time (s)	Overshoot (%)	Settling Time (s)
Tuned	1.04	0.902	9.18
Block	1.72	7.79	24.3

Based on Table 4 above, the tuned PID application shows better results than the block PID, especially in rise time and overshoot parameters. In this research, overshoot is the most concerning parameter that needs to be considered for grasping objects by the prosthetic robot arm—higher overshoot results in over grasping force than the actual optimum force required to grasp an object. The grasped object is deformed during grasping. As for this research, overshoot is the most concerning parameter. High overshoot provides a more significant grasping force as the prosthetic robot arm may deform or crush the grasped object [31].

C. Experiment with Grasping Objects

Fig.19 shows (a) a random cube object that has been grasped, (b) a plastic ball that is grasped, (c) a plastic made hexagon shape solid object, and (d) a wood made cylinder shape solid object.

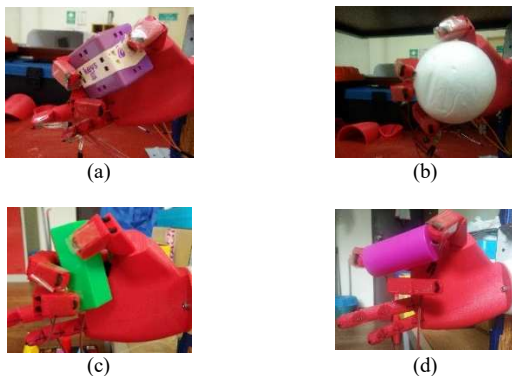


Fig. 19 (a) cube; (b) plastic ball; (c) hexagon; (d) cylinder

The grasping experiment is categorised into three experiments:

- Different shapes with different weights (random objects)
- Same material with different shape
- Same shape with different mass

In experiment 1, random solid objects with random mass were grasped. In experiment 2, objects with the same material but different shapes are grasped for plastic and wood. For experiment 3, objects with the same shape with different masses are grasped. Solid objects with the same shape but different masses are obtained to counter the same condition shape but different manufacturing materials. The two groups of solid objects are made of plastic and wood. In general, wood is higher in mass compared to plastic materials there. The weight of the solid object is different, although the object has the same shape and dimension. Each experiment is carried out for ten repetitions set to measure the mean grasping force by the FSR sensor and the mean static coefficient friction of the object.

D. Experiment 1

Table V shows the grasped objects grasping force. The highest mean grasping force was 1.3397 N for the object of 70g container. The lowest is the solid cube with 0.45775 N. Each object is grasped with various fingers as it depends on the object's physical size. For example, to grasp the puzzle piece, only two fingers are required as the puzzle piece size is smaller than the cylinder container that requires all five fingers to grasp. Figure 20 shows the graph of grasping force versus the objects. In the figure, the mean coefficient friction is different from one object to another as the coefficient friction is inversely proportional to object mass.

TABLE V
GRASPING FORCE DATA OF EXPERIMENT 1

Object	Mass, (g)	Mean Total Grasping Force, (N)	Mean Static coefficient friction, μ_s
Puzzle Piece	54	0.5434	0.10258
Cylinder container	70	1.3397	0.1951
Mini Book	107	0.8459	0.08059
Solid Cube	34	0.45775	0.13724
Plastic Ball	3	0.7155	2.4336
Duck Toy	8	0.4917	0.62638

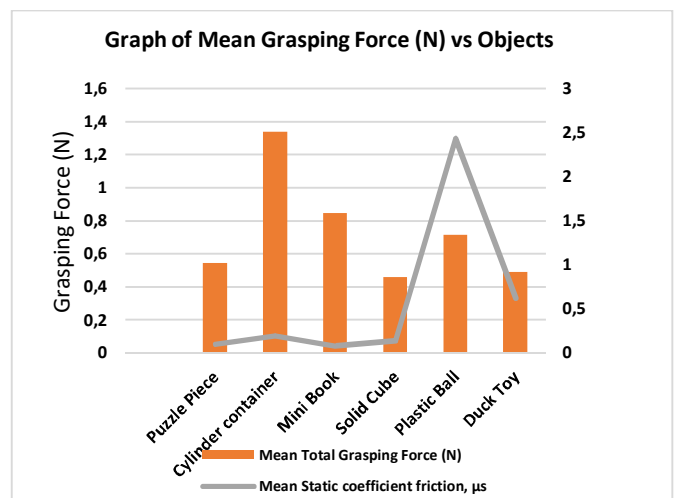


Fig. 20 Grasping force (N) vs type of objects

E. Experiment 2

Table VI shows the mean total grasping force and static coefficient friction of overall plastic shape objects. The mean total grasping force range is between 0.3000 N to 0.5000 N for plastic shape regular objects. On the other hand, in Figure 21, the mean static coefficient friction ranges from 0.4500 to 7.500. Each object has its static friction value as it is inversely proportional to the mass of the object.

TABLE VI
OVERALL DATA OF PLASTICS MADE OBJECTS

Object	Mass, (g)	Mean Total Grasping Force (N)	Mean Static coefficient friction, μ_s
Cube	7	0.3245	0.4725
Cylinder	11	0.3333	3.0884
Hexagon	23	0.3920	1.7373
Pyramid	14	0.4897	3.5656
Rectangular	10	0.4987	5.0834
Square	6	0.4257	7.2317

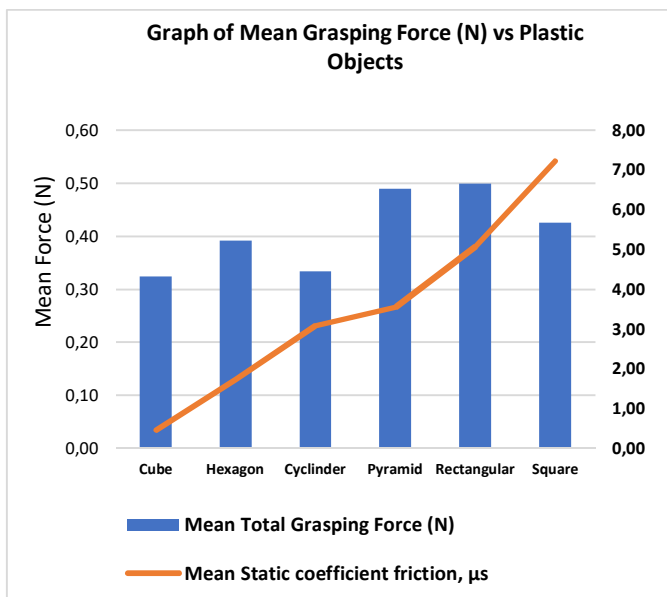


Fig. 21 Mean grasping force versus plastic object shapes

Table VII shows the mean total grasping force and static coefficient friction of overall wood made shape objects. The mean total grasping force range is between 0.3000 N to 0.7000 N for plastic shape regular objects.

TABLE VII
OVERALL DATA OF WOOD MADE OBJECTS

Object	Mass, (g)	Mean Total Grasping Force, (N)	Mean Static coefficient friction, μ_s
Cube	17	0.5288	3.1708
Cylinder	17	0.4711	2.8248
Hexagon	32	0.4339	1.3823
Pyramid	13	0.5058	3.9657
Rectangular	26	0.6388	2.5044
Square	18	0.3363	1.9048

On the other hand, in Figure 22, the mean static coefficient friction ranges from 1.0000 to 4.000. Each object has an independent static friction value as it is inversely proportional to the object's mass.

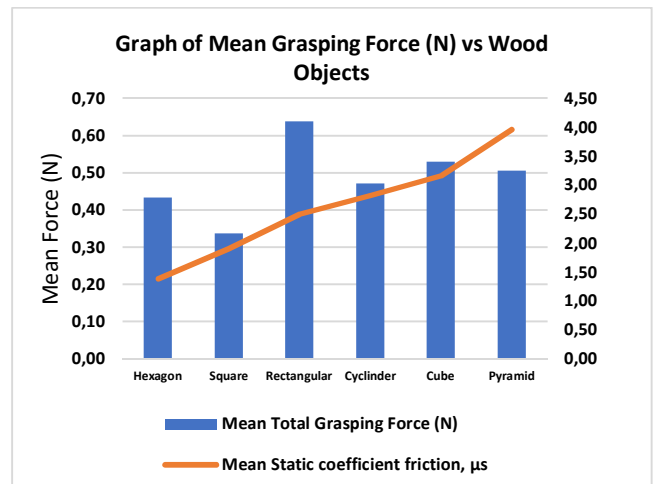


Fig. 22 Mean grasping force versus wood made object shapes

F. Experiment 3

Table VIII shows the collected data of objects with the same shape with different masses. The results proved that objects made of made wood required higher grasping force than plastic-made objects as large grasping is necessary to lift the objects compared to plastic made objects are less heavy in mass than wood made objects. Figure 23 shows the grasp force versus objects. The comparison showed that each object, despite its made material, has different static coefficient friction. For example, the plastic made cube's static coefficient friction is 0.475, but for the wood made cube is 3.1708. Each object has an independent static friction value as it is inversely proportional to the object's mass.

TABLE VIII
OVERALL DATA FOR THE SAME OBJECT WITH DIFFERENT MASS

Object	Mean Total Grasping Force (N)		Mean Static coefficient friction, μ_s	
	Plastic	Wood	Plastics	Wood
Cube	0.3245	0.5288	0.4725	3.1708
Cylinder	0.3333	0.4711	3.0884	2.8248
Hexagon	0.3920	0.4339	1.7373	1.3823
Pyramid	0.4897	0.5058	3.5656	3.9657
Rectangular	0.4987	0.6388	5.0834	2.5044
Square	0.4257	0.3363	7.2317	1.9048

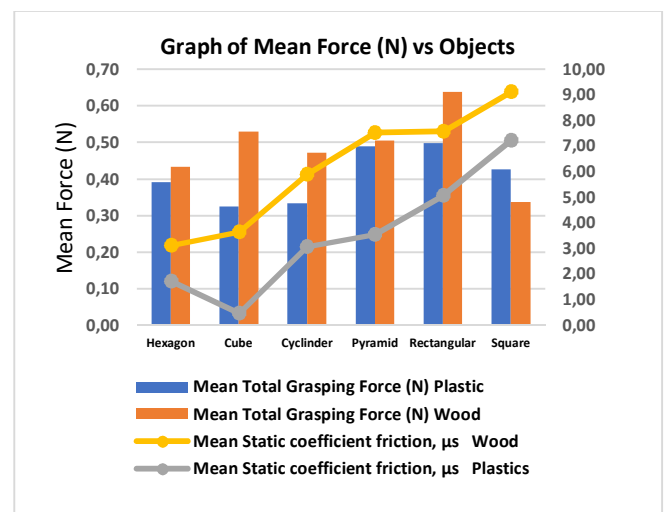


Fig. 23 Force versus objects with different mass

IV. CONCLUSIONS

In this study, a prosthetic robotic arm is successfully fabricated by using a 3D printer with PLA material. The prosthetic robotic arm is with five fingers and connected to two servo motors through nylon strings. There is a limitation to obtaining optimal design and fabrication of the prosthetic robot arm. This is because the 3D printing of the prosthetic requires a precise design, as inaccurate dimensions and angle causes the 3D printer to halter in printing time. Each dimension and angle that merged with another part of the hand such as the forearm to palm, palm to finger must be accurate; the dimension for the installation of the robot arm will be perfectly matched. Else more re-designing and printing time will be required to overcome the in-match issue.

Installing the prosthetic as one piece requires proper equipment and tools such as a soft edge player, a thin screwdriver. Using common hardware tools causes deformation of the PLA material which the hand is printed while placing the components into the forearm of the prosthetic robot arm must be placed with a certain gap. Placing each component, which is close to the other, will cause a short circuit in the hardware. Then, reducing overshoot is the main concern of this study, as it can deform grasping objects if the overshoot value is high. To prevent overshoot in the controller, the PID Autotuning is utilized to reduce overshoot to its optimal value. This study showed that the PID controller with tune application performs better than the block as the gain values can be adjusted to the desired optimum controller performance. The controller performs better in preventing the grasped object's deformation as the overshoot value is 0.902% compared to the previous study.

In this research experiment, regular objects and random objects are grasped to measure the grasping force of the prosthetic robot arm. Based on the experimental results, this study system has successfully grasped objects and measured the grasping force. The difference in total grasping force is the result that based on the contact of the object to the FSR sensor in the fingertip. The amount of contact area for each repetition is the difference from one other. The amount of force of the object that is grasped by the hand varies when in contact with the sensor, depending on the object's position when grasped. For example, suppose the object has a high number of angles and is more dimensionally significant. In that case, the force acting between the object and FSR sensor is higher when in contact than an object with less angle and smaller dimension, which constrains the geometrical error where the fingers are limited to bend to a certain angle only. It is proved in the experiments below. For example, in experiment 1, the puzzle piece is grasped with a servo motor angle of 120° where the mean total grasping force measured is 0.5434 N. However, the mini-book experiment is grasped with a servo angle of 117° , and the mean total grasping force is 0.8459 N. On the other hand, the cylinder container required the servo motor angle of 130° to bend the finger and in contact with the object, but the total amount measured is 1.3397 N. Therefore, the grasping force depends on the position of the object being grasped and the amount of fingers in contact with the object.

In addition, future works on this research can be done by designing the prosthetic robot arm with independent motorized and multi-degree movement of fingers and

fabricated with various materials such as harder material PETG or soft and flexible material TPU. Furthermore, advanced sensors such as muscle or brain sensors can be implemented on the user to have a precise measure of signal from the human body to function the prosthetic robot arm like a real-human hand. Besides that, to realize a prosthetic robotic arm that has better functionality near to human's real hand, experimental and simulation works related with the study of grasping mechanism on uneven surfaces of the grasped object and slippage detection on the grasped object will be executed.

ACKNOWLEDGMENT

The authors thank the Ministry of Higher Education for providing financial support under Fundamental Research Grant Scheme FRGS/1/2019/TK04/UMP/02/15 (University Reference: RDU1901199) and University Malaysia Pahang for laboratory facilities as well as additional financial support under Internal Research grant PGRS210336.

REFERENCES

- [1] N. N. Unanyan and A. A. Belov, "Low-Price Prosthetic Hand Controlled by EMG Signals," *IFAC-PapersOnLine*, vol. 54, no. 13, pp. 299–304, Jan. 2021, doi: 10.1016/J.IFACOL.2021.10.463.
- [2] J. Andrés-Esperanza, J. L. Iserte-Vilar, I. Llop-Harillo, and A. Pérez-González, "Affordable 3D-printed tendon prosthetic hands: Expectations and benchmarking questioned," *Eng. Sci. Technol. an Int. J.*, vol. 31, p. 101053, Jul. 2022, doi: 10.1016/J.JESTCH.2021.08.010.
- [3] J. Zbinden, E. Lendaro, and M. Ortiz-Catalan, "Prosthetic embodiment: systematic review on definitions, measures, and experimental paradigms," *J. NeuroEngineering Rehabil.* 2022 191, vol. 19, no. 1, pp. 1–16, Mar. 2022, doi: 10.1186/S12984-022-01006-6.
- [4] N. Gorman, J. Feng, and S. Y. Marin Pareja, "Enhancing Prosthetic Hand Functionality with Elastic 3D-Printed Thermoplastic Polyurethane," *Lect. Notes Networks Syst.*, vol. 263, pp. 183–190, 2021, doi: 10.1007/978-3-030-80744-3_23.
- [5] M. Orellana-Donoso, J. J. Valenzuela-Fuenzalida, M. Gold-Semmler, Guernica-Garcia-Gorigoitia, R. Shane-Tubbs, and E. Santana-Machuca, "Neural entrapments associated with musculoskeletal anatomical variations of the upper limb: Literature review," *Transl. Res. Anat.*, vol. 22, p. 100094, Jan. 2021, doi: 10.1016/J.TRIA.2020.100094.
- [6] M. A. Voutsalath, C. K. Bichakjian, F. Pelosi, D. Blum, T. M. Johnson, and P. M. Farrehi, "Electrosurgery and implantable electronic devices: Review and implications for office-based procedures," *Dermatologic Surg.*, vol. 37, no. 7, pp. 889–899, Jul. 2011, doi: 10.1111/J.1524-4725.2011.02006.X.
- [7] J. Zuniga *et al.*, "Cyborg beast: A low-cost 3d-printed prosthetic hand for children with upper-limb differences," *BMC Res. Notes*, vol. 8, no. 1, Dec. 2015, doi: 10.1186/S13104-015-0971-9.
- [8] D. Babu, A. Nasir, A. S. Jamaludin, and M. H. Rosle, "Holding, Grasping and Sensing of Prosthetic Robot Arm Like a Real Human Hand, a Journey Beyond Limits: An Extensive Review," pp. 485–504, 2022, doi: 10.1007/978-981-16-4115-2_39.
- [9] A. Gonzalez, L. Garcia, J. Kilby, and P. McNair, "Robotic devices for paediatric rehabilitation: a review of design features," *Biomed. Eng. Online*, vol. 20, no. 1, pp. 1–33, 2021, doi: 10.1186/s12938-021-00920-5.
- [10] T. Singh, S. Kumar, and S. Sehgal, "3D printing of engineering materials: A state of the art review," *Mater. Today Proc.*, vol. 28, pp. 1927–1931, 2020, doi: 10.1016/J.MATPR.2020.05.334.
- [11] F. Šproch, V. Schindlerová, and I. Šajdlerová, "Using 3D printing technology in prototype production to control the dimensions of complexly shaped products," *Manuf. Technol.*, vol. 20, no. 3, pp. 385–393, 2020, doi: 10.21062/mft.2020.061.
- [12] A. J. Sterkenburg *et al.*, "Quality of life of patients with 3D-printed arm prostheses in a rural area of Sierra Leone," *Heliyon*, vol. 7, no. 7, p. e07447, Jul. 2021, doi: 10.1016/J.HELIYON.2021.E07447.
- [13] M. Ortiz-Catalan, E. Mastinu, C. M. Greenspon, and S. J. Bensmaia, "Chronic Use of a Sensitized Bionic Hand Does Not Remap the Sense of Touch," *Cell Rep.*, vol. 33, no. 12, p. 108539, Dec. 2020, doi: 10.1016/J.CELREP.2020.108539.

- [14] A. Mehman Sefat, S. Ahmad, A. Angleraud, E. Rahtu, and R. Pieters, "Robotic grasping in agile production," *Deep Learn. Robot Percept. Cogn.*, pp. 407–433, Jan. 2022, doi: 10.1016/B978-0-32-385787-1.00021-X.
- [15] S. Nojiri, A. Yamaguchi, Y. Suzuki, T. Tsuji, and T. Watanabe, "Sensing and Control of Friction Mode for Contact Area Variable Surfaces (Friction-variable Surface Structure)," *2020 3rd IEEE Int. Conf. Soft Robot. RoboSoft 2020*, pp. 215–222, May 2020, doi: 10.1109/ROBOSOFT48309.2020.9116019.
- [16] R. R. Devaraja, R. Maskeliūnas, and R. Damaševičius, "Design and Evaluation of Anthropomorphic Robotic Hand for Object Grasping and Shape Recognition," *Comput. 2021, Vol. 10, Page 1*, vol. 10, no. 1, p. 1, Dec. 2020, doi: 10.3390/COMPUTERS10010001.
- [17] M. D. Twardowski, S. H. Roy, Z. Li, P. Contessa, G. De Luca, and J. C. Kline, "Motor unit drive: A neural interface for real-time upper limb prosthetic control," *J. Neural Eng.*, vol. 16, no. 1, Feb. 2019, doi: 10.1088/1741-2552/AABE0F.
- [18] U. Wijk, I. K. Carlsson, C. Antfolk, A. Björkman, and B. Rosén, "Sensory Feedback in Hand Prostheses: A Prospective Study of Everyday Use," *Front. Neurosci.*, vol. 14, p. 663, Jul. 2020, doi: 10.3389/FNINS.2020.00663/BIBTEX.
- [19] L. F. Engels, A. W. Shehata, E. J. Scheme, J. W. Sensinger, and C. Cipriani, "When less is more-discrete tactile feedback dominates continuous audio biofeedback in the integrated percept while controlling a myoelectric prosthetic hand," *Front. Neurosci.*, vol. 13, no. JUN, 2019, doi: 10.3389/FNINS.2019.00578.
- [20] M. Rossi, M. Bianchi, E. Battaglia, M. G. Catalano, and A. Bicchi, "HapPro: A Wearable Haptic Device for Proprioceptive Feedback," *IEEE Trans. Biomed. Eng.*, vol. 66, no. 1, pp. 138–149, Jan. 2019, doi: 10.1109/TBME.2018.2836672.
- [21] S. F. Ahmed, M. H. Tanveer, I. J. Kiwarkis, and H. B. Basy, "Design and controlling of low-cost prosthetic hand using force sensor," *Proc. - 3rd Int. Conf. Inf. Comput. Technol. ICICT 2020*, pp. 347–350, 2020, doi: 10.1109/ICICT50521.2020.00061.
- [22] Novi Rahayu, "View of Early Warning Of Leaking Lpg Gas Through Short Message Service (Sms) And Loudspeaker Tool Using Arduino Uno," *Journal of Applied Engineering and Technological Science Vol 1(2) 2020: 91-102*, 2020. <https://journal.yrpiiku.com/index.php/jaets/article/view/61/36> (accessed Apr. 24, 2022).
- [23] K. S. Kaswan, S. P. Singh, and S. Sagar, "Role of Arduino in real world applications," *Int. J. Sci. Technol. Res.*, vol. 9, no. 1, pp. 1113–1116, 2020.
- [24] A. K. Aneesha, S. Bhat, and M. Kanthi, "Load Cell and FSR-Based Hand-Assistive Device," *Adv. Intell. Syst. Comput.*, vol. 1198, pp. 148–156, 2021, doi: 10.1007/978-981-15-6584-7_15.
- [25] D. Esposito *et al.*, "A Piezoresistive Sensor to Measure Muscle Contraction and Mechanomyography," *Sensors 2018, Vol. 18, Page 2553*, vol. 18, no. 8, p. 2553, Aug. 2018, doi: 10.3390/S18082553.
- [26] Liu Jun, "Design and Research of Servo Motor Control System Based on Stm32 Single Chip Microcomputer | Solid State Technology," *Solid State Technology Vol. 63 No. 3 (2020)*, 2020. <http://solidstatetechnology.us/index.php/JSST/article/view/3681> (accessed Apr. 24, 2022).
- [27] A. A. Kadhum and M. M. Abdulhussein, "Implementation dc motor as servomotor by using arduino and optical rotary encoder," *Mater. Today, Proc.*, Apr. 2021, doi: 10.1016/J.MATPR.2021.03.576.
- [28] D. C. Adam Maxwell Doumin1, Zul Hilmi Che Daud2,*, Zainab Asus2, Izhari Izmi Mazali1, Mohd Kameil Abdul Hamid1, Mohd Farid Muhamad Said2, "Recent Studies on Lithium-ion Battery Thermal Behaviour for Electric and Hybrid Electric Vehicles: A Review | Journal of Advanced Research in Fluid Mechanics and Thermal Sciences," *Journal of Advanced Research in Fluid Mechanics and Thermal Sciences* 61, Issue 2(2019) 262-272, 2019. <https://www.akademiabaru.com/submit/index.php/arfmts/article/view/2678> (accessed Apr. 24, 2022).
- [29] M. Abdelbaky, J. R. Peeters, S. Van den Eynde, I. Zaplana, and W. Dewulf, "A comparative assessment of resource-use criticality in advanced lithium-ion battery technologies," *Procedia CIRP*, vol. 105, pp. 7–12, Jan. 2022, doi: 10.1016/J.PROCIR.2022.02.002.
- [30] I. Llop-Harillo, A. Pérez-González, J. Starke, and T. Asfour, "The Anthropomorphic Hand Assessment Protocol (AHAP)," *Rob. Auton. Syst.*, vol. 121, p. 103259, 2019, doi: 10.1016/j.robot.2019.103259.
- [31] A. Prakash and S. Sharma, "A low-cost system to control prehension force of a custom-made myoelectric hand prosthesis," *Res. Biomed. Eng.*, vol. 36, no. 3, pp. 237–247, 2020, doi: 10.1007/s42600-020-00064-w.